Nonlinear Digital Cancellation in Full-Duplex Devices using Spline-Based Hammerstein Model

Pablo Pascual Campo, Dani Korpi, Lauri Anttila, and Mikko Valkama

Laboratory of Electronics and Communications Engineering, Tampere University of Technology, Finland
e-mail: pablo.pascualcampo@tut.fi, dani.korpi@tut.fi, lauri.anttila@tut.fi, mikko.e.valkama@tut.fi

***Abstract*—In this paper, a novel digital self-interference canceller based on a Hammerstein adaptive filter is proposed and examined. The proposed system consists of a spline-interpolated lookup table to model the nonlinear power amplifier, followed by a linear filter accounting for the impulse response of the linear self-interference channel. The gradient descent based parameter learning algorithms are derived, which estimate the spline control points and the filter coefficients in a decoupled manner. The proposed digital canceller leads to a complexity reduction of 77% when compared to the existing state-of-the-art solutions. Performance evaluations using measured data from a complete inband full-duplex prototype system operating at 2.4 GHz ISM band show the effectiveness of the proposed technique, demonstrating that it obtains similar cancellation performance as the existing state-of-the-art canceller, regardless of its lower complexity. The measured digital self-interference cancellation values are 45 dB, 43 dB and 38 dB with 20 MHz, 40 MHz and 80 MHz channel bandwidths, respectively. These results indicate that the complexity-accuracy trade-off of the proposed decoupled spline-based cancellation approach is very favorable. Owing to the resulting decrease in the computational complexity, the proposed digital cancellation technique brings inband full-duplex transceivers one step closer to commercial deployments.**

***Index Terms*—Spline interpolation, inband full-duplex, decoupled model, self interference, digital cancellation, nonlinear distortion, adaptive tracking**

I. Introduction

The practical feasibility of inband full-duplex communications, where individual radio devices transmit and receive simultaneously on the same frequency channel, has recently been proven by various research groups [1]–[5]. The main motivation for implementing such inband full-duplex systems stems from the resulting increase in spectral efficiency; the simultaneous transmission and reception facilitates a twofold increase in the data rate without requiring any additional bandwidth. Such an improvement is highly sought after especially in the heavily congested ultra high frequency (UHF) bands, and may turn out to be a key technology in the future wireless networks.

However, in order to make inband full-duplex technology commercially feasible, the problem of self-interference (SI) must be dealt with in an efficient manner [6], [7]. The SI is caused by the own transmit signal overlapping the desired received signal both temporally and spectrally due to the inband full-duplex operation, and the full-duplex device must be capable of suppressing it in order to operate properly. In principle, this can be done by subtracting the known transmit signal from the received signal, after accounting for the effects of the coupling channel. Since any full-duplex device must inevitably perform the SI cancellation procedure, it is crucial to explore ways of minimizing the involved computational complexity, while at the same time being able to provide the needed SI cancellation performance.

In this paper, we propose a novel digital SI cancellation solution, which utilizes an adaptive Hammerstein filter while modeling the nonlinearity with splines to significantly reduce the computational complexity compared to existing state-of-the-art solutions. In particular, we extend the real-valued spline adaptive filters from [8] to complex-valued form, and derive decoupled adaptive learning rules for the spline control points and the linear filter. To the best of our knowledge, this type of a spline-based digital SI canceller has not been proposed in the earlier literature.

Compared to the state-of-the-art solutions [2], [4], the proposed digital canceller achieves the same cancellation performance with 77% fewer computations. This is proven by evaluating the proposed canceller with measured SI signals from a complete inband full-duplex prototype system operating at 2.4 GHz ISM band and comparing its performance to that of the earlier solutions. The obtained results show that the spline-based Hammerstein digital canceller is a promising solution for bringing the inband full-duplex technology one step closer to a commercially viable implementation, with a very favorable cancellation performance–complexity trade-off.

The rest of this paper is organized as follows. In Section II, the proposed spline-based digital canceller is described, alongside with the parameter adaptation rules. Section III provides analysis of the computational complexity together with complexity comparison against a memory polynomial-based digital canceller, which represents the current state-of-the-art. After this, the performance of the digital cancellers is evaluated and compared in Section IV using measurement data. Finally, Section V concludes the paper.

Notation used in this paper

In this paper, vectors are represented with boldface lowercase letters. By default, all vectors consist of complex-valued elements represented as columns vectors (i.e., $\mathbf{x} \in \mathbb{C}^{N\times 1} = [x_0 \; x_1 \; \cdots \; x_{N-1}]^T$). Matrices are expressed with boldface capital letters (i.e., $\mathbf{A} \in \mathbb{C}^{N\times M}$). Ordinary transpose and Hermitian transpose of vectors are represented as $(\cdot)^T$ and $(\cdot)^H$, respectively. Moreover, the absolute value and floor operator are denoted by $|\cdot|$ and $\lfloor\cdot\rfloor$, respectively.

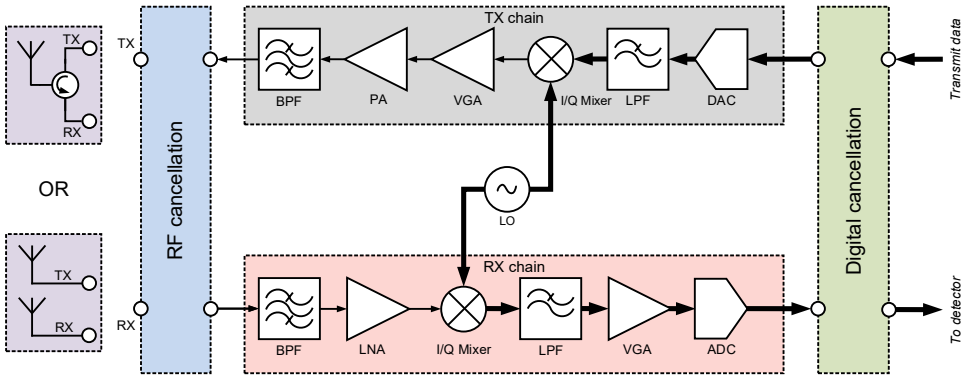

Fig. 1: Considered inband full-duplex device architecture.

II. System Model and Proposed Spline-based Canceller

A. Principles of Spline Interpolation

In spline interpolation, particular type of piece-wise polynomials under continuity and smoothness constraints are used to interpolate the input data [9]. With this technique, a nonlinear system can be modeled accurately even when using low-order piece-wise polynomials, as opposed to conventional polynomial models, where high orders are usually needed. The piece-wise polynomials are controlled through a set of control points being adapted according to the nonlinearity present in the system.

Spline curves can be generalized to any piece-wise degree, denoted here by P_{SP}. The spline curve is therefore a combination of $P_{\mathrm{SP}}+1$ spline segments between so-called knots, which define the boundaries of the individual splines. The individual region between the ith and $i+1$th knot is defined as the ith span. Moreover, each spline curve is characterized by a P_{SP}th-degree spline basis function $p_i^{P_{\mathrm{SP}}}(u_n)$, which is defined as [10]

$$p_i^{P_{\mathrm{SP}}}(u_n) = \frac{q_{i+P_{\mathrm{SP}}+1} - u_n}{q_{i+P_{\mathrm{SP}}+1} - q_{i+1}} p_{i+1}^{P_{\mathrm{SP}}-1}(u_n) + \frac{u_n - q_i}{q_{i+P_{\mathrm{SP}}} - q_i} p_i^{P_{\mathrm{SP}}-1}(u_n), \tag{1}$$

where q_i is the control point for the ith span. The abscissa value and the span are defined as

$$u_n = \frac{x[n]}{\Delta x} - \left\lfloor \frac{x[n]}{\Delta x} \right\rfloor, \tag{2}$$

$$i_n = \left\lfloor \frac{x[n]}{\Delta x} \right\rfloor + \frac{Q-1}{2}, \tag{3}$$

where $x[n]$ is the input signal of the spline system, Δx is the uniform distance between the consecutive knots, and Q is the total number of knots.

This function can be obtained recursively, starting from the spline polynomial of degree $P_{\mathrm{SP}} = 0$, defined as

$$p_i^0(u) = \begin{cases} 1 & \text{if } q_i \le u < q_{i+1}, \\ 0 & \text{otherwise.} \end{cases} \tag{4}$$

For a more detailed explanation, refer, for instance, to [9].

As shown in [10], the output of a spline nonlinearity can be expressed with matrix notation as

$$s_i(u_n) = \mathbf{S}_n \mathbf{q}_n, \tag{5}$$

where $\mathbf{q}_n \in \mathbb{R}^{Q\times 1} = [q_0 \;\; q_1 \;\; \cdots \;\; q_{Q-1}]^T$ is a real-valued vector containing the control points and $\mathbf{S}_n \in \mathbb{R}^{1\times Q}$ is defined as

$$\mathbf{S}_n = [0 \;\cdots\; 0 \; \mathbf{u}_n^T\mathbf{C} \; 0 \;\cdots\; 0]. \tag{6}$$

Here, $\mathbf{u}_n^T\mathbf{C}$ represents the matrix multiplication between the abscissa vector $\mathbf{u}_n \in \mathbb{R}^{(P_{\mathrm{SP}}+1)\times 1} = [u_n^{P_{\mathrm{SP}}} \; u_n^{P_{\mathrm{SP}}-1} \; \cdots \; 1]^T$ and the spline basis matrix $\mathbf{C} \in \mathbb{R}^{(P_{\mathrm{SP}}+1)\times(P_{\mathrm{SP}}+1)}$, which is pre-computed and fixed. The resulting $(P_{\mathrm{SP}}+1)\times 1$ vector is then sorted in $\mathbf{S}_n$ starting from the span index i in the current iteration. This way, $\mathbf{u}_n^T\mathbf{C}$ is multiplied with the correct samples of $\mathbf{q}_n$ in the ith span. The spline basis matrix $\mathbf{C}$ is dependent on the type of splines used, as well as on the spline polynomial order. For example, for B-splines and $P_{\mathrm{SP}} = 2$, the spline basis matrix becomes [10]

$$\mathbf{C} = \frac{1}{2}\begin{bmatrix} 1 & -2 & 1 \\ -2 & 2 & 0 \\ 1 & 1 & 0 \end{bmatrix}. \tag{7}$$

B. Proposed Spline-Based Hammerstein Canceller

The objective of the proposed canceller is to accurately reconstruct nonlinearly distorted SI within a full-duplex device whose block diagram is depicted in Fig. 1. Previous works in [2], [7], [11] have shown that Hammerstein-type models are, in general, accurate in reconstructing nonlinearly distorted SI but they involve substantial processing complexity. To this end, we propose using a decoupled Hammerstein model, which consists of a static nonlinearity representing the nonlinear power amplifier (PA), followed by a linear filter which models the linear SI channel. This linear SI channel includes the PA memory as well as the the overall linear coupling response from the PA output to the receiver digital baseband.

The proposed spline-interpolated lookup table for modeling and cancelling the SI is illustrated in Fig. 2, where the signal $x[n]$ corresponds to the input signal of the proposed structure,

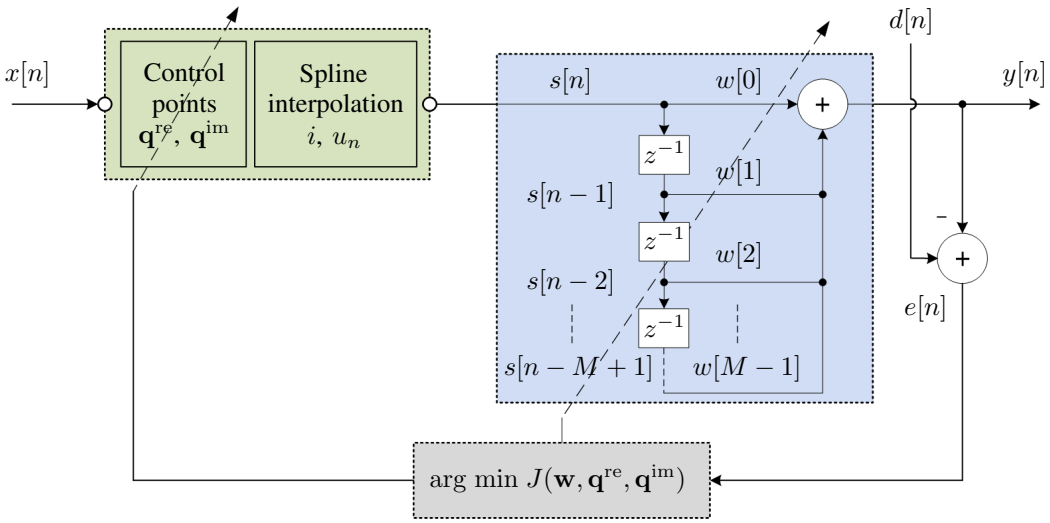

Fig. 2: Architecture of the proposed nonlinear decoupled spline-based Hammerstein self-interference canceller. Note that the pre-cursor taps are omitted from the diagram for clarity.

in this case the original transmit signal. However, this signal is complex-valued, whereas regular splines are real-valued. Since here the splines are used to model the nonlinear response of the PA, which only depends on the magnitude of the input signal, the real-valued splines can be used to model it by defining separate splines for the I and Q components and using $|x[n]|$ as the input of both splines. Consequently, the abscissa and span of both splines is now obtained by replacing $x(n)$ with $|x(n)|$ in (2) and (3), and omitting the term $\frac{Q-1}{2}$ from (3) as the abscissa is now non-negative. The splines modeling the real and imaginary (the I and Q) responses of the PA are therefore expressed as

$$s_1(u_n) = \mathbf{S_n}(1 + \mathbf{q}_n^{\mathrm{re}}), \tag{8}$$

$$s_2(u_n) = \mathbf{S}_n\mathbf{q}_n^{\mathrm{im}}, \tag{9}$$

where $\mathbf{q}_n^{\mathrm{re}}$ and $\mathbf{q}_n^{\mathrm{im}}$ contain the control points for the nth iteration.

By using the expression in (8) and (9), the complex-valued output of the nonlinear system can be written as

$$s[n] = x[n]\mathbf{S}_n(1 + \mathbf{q}_n^{\mathrm{re}} + j\mathbf{q}_n^{\mathrm{im}}) = x[n]\mathbf{S}_n(1 + \mathbf{q}_n), \tag{10}$$

where $\mathbf{q}_n$ is the overall complex-valued control point vector for the nth iteration. The signal $s[n]$ retains the phase information of the original signal via the multiplication by $x[n]$, while the two splines determine the real and imaginary responses of the nonlinear PA.

Compared to (5), we now define the control point vector $\mathbf{q}_n$ as a deviation from 1. This has several benefits, especially in the current application. First, if $\mathbf{q}_n$ is initialized as a zero vector, the spline will be linear (i.e., $s[n] = x[n]$) in the beginning of the algorithm learning period. This will effectively remove the gain ambiguity between the two blocks (linear filter and splines), and the linear filter will immediately start to converge to a state where it handles the gain. A second benefit is that the dynamic range of $\mathbf{q}_n$ is reduced, and thus a smaller number of bits is required in a fixed-point implementation.

In addition to the nonlinear distortion, also the memory effects need to be modeled. This includes the memory of the PA itself as well as the linear response of the rest of the overall SI channel, from PA output all the way to the receiver baseband. Considering this, the final output signal of the model is

$$y[n] = \mathbf{w}_n^H \mathbf{s}_n, \tag{11}$$

where $\mathbf{w}_n$ is the impulse response of the linear filter, defined as $\mathbf{w}_n \in \mathbb{C}^{M\times 1} = [w_n[0]\ w_n[1]\ \cdots\ w_n[M-1]]^T$, $\mathbf{s}_n \in \mathbb{C}^{M\times 1} = [s[n+M_{\mathrm{pre}}]\ \cdots\ s[n]\ \cdots\ s[n-M_{\mathrm{post}}]]^T$, M_{pre} is the number of pre-cursor taps, M_{post} is the number of post-cursor taps, and $M = M_{\mathrm{pre}} + M_{\mathrm{post}} + 1$.

C. Derivation of the Learning Rules

In order to estimate the unknown parameters of the system, namely the linear filter $\mathbf{w}_n$, and the control points $\mathbf{q}_n$, let us consider the error signal

$$e[n] = d[n] - y[n], \tag{12}$$

where $d[n]$ denotes the observed SI signal at receiver digital baseband, which the digital canceller aims at suppressing. At this point, the problem lies in estimating the values of the linear filter and the spline control points to minimize the error signal $e[n]$. This can be done by using the basic gradient descent solution, where the quantities are learned by adjusting them to the negative direction of the gradient of the cost function. Furthermore, to obtain a simple learning rule, only the instantaneous gradient is used, similar to the classical least mean squares (LMS) filter.

For the estimation of the memory model, the cost function is defined as the instantaneous squared error, expressed as

$$J(\mathbf{w}_n, \mathbf{q}_n) = e[n]e^*[n]. \tag{13}$$

It can then be noted that the memory is after the nonlinearity, and therefore the splines are not dependent on $\mathbf{w}_n$. As a result, the system with respect to $\mathbf{w}_n$ is simply a linear filter, where the traditional LMS learning rule can be used. Consequently, the learning rule for the memory filter becomes

$$\mathbf{w}_{n+1} = \mathbf{w}_n - \mu_{\mathrm{w}} \frac{\partial J(\mathbf{w}_n, \mathbf{q}_n)}{\partial \mathbf{w}_n} = \mathbf{w}_n + \mu_{\mathrm{w}} e^*[n]\mathbf{s}_n, \tag{14}$$

where μ_{w} is the learning step-size.

The complex-valued control-points can be learned using a similar rule, which can be expressed as

$$\mathbf{q}_{n+1} = \mathbf{q}_n - \mu_{\mathrm{q}} \frac{\partial J(\mathbf{w}_n, \mathbf{q}_n)}{\partial \mathbf{q}_n}, \tag{15}$$

where μ_{q} is the corresponding step-size. However, now the partial derivative is not previously known, and must be calculated in order to express the learning rule. Firstly, we can rewrite it as [12]:

$$\begin{aligned}
\frac{\partial J(\mathbf{w}_n, \mathbf{q}_n)}{\partial \mathbf{q}_n} &= e^*[n]\frac{\partial e[n]}{\partial \mathbf{q}_n} + e[n]\frac{\partial e^*[n]}{\partial \mathbf{q}_n} \\
&= -e^*[n]\frac{\partial y[n]}{\partial \mathbf{q}_n} - e[n]\frac{\partial y^*[n]}{\partial \mathbf{q}_n} \\
&= -e^*[n]\left[\frac{\partial y[n]}{\partial \mathbf{q}_n^{\mathrm{re}}} + j\frac{\partial y[n]}{\partial \mathbf{q}_n^{\mathrm{im}}}\right] \\
&\quad - e[n]\left[\left(\frac{\partial y[n]}{\partial \mathbf{q}_n^{\mathrm{re}}}\right)^* + j\left(\frac{\partial y[n]}{\partial \mathbf{q}_n^{\mathrm{im}}}\right)^*\right].
\end{aligned} \tag{16}$$

Therefore, it suffices to determine the partial derivative of $y(n)$ with respect to the control points of the real and imaginary splines. Invoking elementary differentiation rules, they can be written as

$$\frac{\partial y[n]}{\partial \mathbf{q}_n^{\mathrm{re}}} = \mathbf{\Sigma}_n \mathbf{X}_n \mathbf{w}_n^*, \tag{17}$$

$$\frac{\partial y[n]}{\partial \mathbf{q}_n^{\mathrm{im}}} = j\mathbf{\Sigma}_n \mathbf{X}_n \mathbf{w}_n^*, \tag{18}$$

where $\mathbf{\Sigma}_n \in \mathbb{R}^{Q\times M} = \left[\mathbf{S}_{n+M_{\mathrm{pre}}}^T \ \cdots \ \mathbf{S}_n^T \ \cdots \ \mathbf{S}_{n-M_{\mathrm{post}}}^T\right]$, and $\mathbf{X}_n = \mathrm{diag}\left\{x[n+M_{\mathrm{pre}}], \ \ldots, \ x[n-M_{\mathrm{post}}]\right\}$.

Substituting these into (16), the partial derivative becomes

$$\frac{\partial J(\mathbf{w}_n, \mathbf{q}_n)}{\partial \mathbf{q}_n} = -2e(n)\mathbf{\Sigma}_n \mathbf{X}_n^* \mathbf{w}_n. \tag{19}$$

Therefore, the learning rule of the control points can finally be written as

$$\mathbf{q}_{n+1} = \mathbf{q}_n + \mu_{\mathrm{q}} e(n)\mathbf{\Sigma}_n \mathbf{X}_n^* \mathbf{w}_n. \tag{20}$$

During the actual operation of the proposed canceller, both the linear filter and the control points are then estimated and updated in parallel as per (14) and (20).

The downside of the update in (20) is the high complexity in computing $\mathbf{\Sigma}_n \mathbf{X}_n^* \mathbf{w}_n$, especially if the filter $\mathbf{w}_n$ is long. However, the larger tap values of $\mathbf{w}_n$ are clearly the most significant ones in the update, and these tap values are usually those around the index $M_{\mathrm{pre}} + 1$. Thus, as a simplifying approximation, we propose to reduce the time span of the matrices, keeping only the entries corresponding to the most significant taps in $\mathbf{w}_n$. This way, the computation of $\mathbf{\Sigma}_n \mathbf{X}_n^* \mathbf{w}_n$ can be greatly simplified.

III. Computational Complexity Analysis

A. Complexity of Proposed Canceller

Let us next briefly consider the computational complexity of the proposed decoupled spline-based Hammerstein algorithm. For this purpose, the number of arithmetical operations required to run a single iteration of the algorithm is calculated, in a similar manner as done in [13]. However, for brevity, herein we only consider the number of multiplications since the computational cost of additions is negligible in comparison.

The complexity of the algorithm can be detailed based on the cancellation processing steps performed in each iteration.

- At the beginning of each iteration, the span index and the abscissa value (i_n and u_n) are computed. For this, it is necessary to calculate the absolute value of a complex number, whose analytical expression contains a square root. To avoid such a costly operation, the absolute value can be approximated as in [14]:

$$\begin{aligned}
|x[n]| = \alpha \ &\max\left\{|\mathrm{Re}\{x[n]\}|, |\mathrm{Im}\{x[n]\}|\right\} \\
&+ \beta \ \min\left\{|\mathrm{Re}\{x[n]\}|, |\mathrm{Im}\{x[n]\}|\right\},
\end{aligned} \tag{21}$$

  where α and β can be chosen based on selected approximation criterion, such as minimum RMS error for zero-mean signals.
- Next, the signals $s[n]$ and $y[n]$ must be calculated, as per (10) and (11).

Then, in order to update the coefficients of the learning rates, the following steps are followed:

- The linear filter $\mathbf{w}_{n+1}$ is updated as shown in (14).
- Finally, the control point vector $\mathbf{q}_{n+1}$ is updated according to (20). In the analysis we consider a time span of $\tau = 5$ taps for $\mathbf{w}_n$. This will considerably reduce the computational complexity of the vector update with an acceptable loss of cancellation.

The corresponding numbers of required multiplications per one iteration are collected in Table I. Note that in some cases it might not be necessary to update all the coefficients in each iteration, which obviously reduces the overall computational cost. In particular, as discussed below, it is often unnecessary to continuously update the spline control points as the nonlinear characteristics of the PA remain relatively constant over time.

B. Complexity of Memory Polynomial Canceller

The widely used memory polynomial (MP) model constitutes the current state of the art when modeling the behaviour of PAs in the context of inband full-duplex devices [2], [7], [11]. For this reason, it has been adopted as the reference benchmark for the proposed novel solution. Below, we shortly

TABLE I: Number of required arithmetic operations in each iteration of the spline-based digital cancellation algorithm.

Computation		Real multiplications
Cancellation	$s[n], y[n]$	$(P_{\mathrm{SP}}+1)^2+P_{\mathrm{SP}}+2Q+3M+4$
Coefficient updates	$\mathbf{w}_{n+1}$	$3M+2$
	$\mathbf{q}_{n+1}$	$Q(2\mathcal{T}+3)+3\mathcal{T}+2$
Total		$P_{\mathrm{SP}}(P_{\mathrm{SP}}+3)+\mathcal{T}(2Q+3)+5Q+6M+9$

review the principal processing structure of such MP-based digital SI canceller and address its computational complexity for reference.

The discrete-time MP model can be expressed as

$$y[n]=\sum_{\substack{p=1\\ p\ \mathrm{odd}}}^{P_{\mathrm{MP}}}\sum_{m=-M_{\mathrm{pre}}}^{M_{\mathrm{post}}}h_p[m]\psi_p[x[n-m]], \qquad (22)$$

where P_{MP} is the nonlinearity order of the MP model, $h_p[m]$ represents the overall effective coupling channel from the pth basis function perspective, and $\psi_p[x[n]]=|x[n]|^{p-1}x[n]$ is the pth-order basis function. In addition, in this model these basis functions need to be prewhitened or orthogonalized to ensure efficient learning [7]. After this step, the parameters of the MP model can be learned with the basic LMS algorithm, the use of which facilitates a fair comparison with the proposed solution. Such an algorithm is described in [11], wherein further details can be found. The total number of arithmetic operations can easily be calculated as $3(\frac{P_{\mathrm{MP}}+1}{2})^2+(3M+1)(P_{\mathrm{MP}}+1)+2$ real multiplications per one iteration, of which $3(\frac{P_{\mathrm{MP}}+1}{2})^2+(3M+2)(\frac{P_{\mathrm{MP}}+1}{2})$ are used for the actual cancellation processing while the coefficient updates require $3M(\frac{P_{\mathrm{MP}}+1}{2})+2$ real multiplications.

C. Comparison

For the purpose of comparing the aforementioned models, typical parameter values are chosen in accordance with the characteristics of each algorithm. When considering the decoupled spline-based Hammerstein model, the degree of the polynomial is chosen as $P_{\mathrm{SP}}=2$, which is sufficient to reach a SI cancellation performance similar to that of the MP model (see Section IV). The total number of knots is chosen as $Q=11$, and the time span for the matrix simplification is $\tau=5$. The overall memory length of the linear filter is chosen for both models as $M=M_{\mathrm{pre}}+M_{\mathrm{post}}+1=25+50+1=76$. Consequently, using Table I, the amount of computations per iteration can be calculated as 655 real multiplications for the proposed decoupled Hammerstein algorithm. Of this, the cancellation processing accounts for only 265 real multiplications.

As for the MP-based canceller, $P_{\mathrm{MP}}=11$ is chosen as the order of the nonlinearity, similar to [11]. As a result, the number of real multiplications to be performed within an iteration is 2858, according to the expression provided in the previous subsection. This demonstrates the large complexity reduction when using the novel decoupled spline-based Hammerstein approach, as nearly 77% less multiplications per iteration suffices to obtain a comparable cancellation performance. Moreover, when considering only the actual cancellation processing, the number of real multiplications per iteration is 1488 for the MP canceller. Therefore, under static conditions where it is not necessary to update any of the coefficients, the spline-based canceller can operate with 82% fewer multiplications.

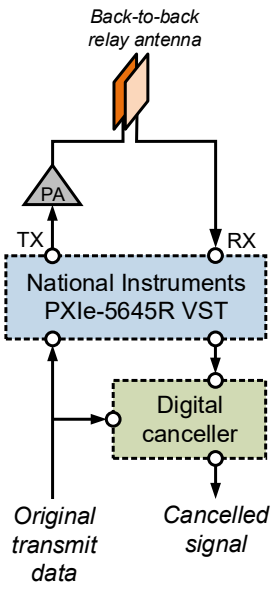

Fig. 3: Illustration of the overall RF measurement setup used in obtaining the evaluation data.

However, in most practical cases, while the nonlinear behaviour of the PA remains more or less static, the wireless coupling channel is time-variant and the corresponding coefficients must be adapted continuously. This unveils another benefit of the proposed decoupled spline-based solution, as it considers the PA nonlinearity and the linear channel as separate entities, meaning that the channel coefficients can be updated while the spline control points are kept static after the initial learning phase. Taking this into account, it suffices for the proposed decoupled spline-based model to update only the memory filter during the actual operation, reducing the number of real multiplications per iteration to 495 with the example parameters. Recognizing that it is not possible to separate the effects of the linear coupling channel and the PA nonlinearity in the MP model, under this assumption the proposed spline-based canceller can operate with 82% fewer multiplications.

IV. Experimental results

In order to evaluate the cancellation performance of the proposed spline-based digital canceller, a similar RF measurement environment as in [4], reflecting a complete inband full-duplex prototype system, is used. The measured data consists of the observed SI signal obtained using the system depicted in Fig. 3, where a back-to-back relay antenna is used to provide the transmitter-receiver isolation in the analog domain. That

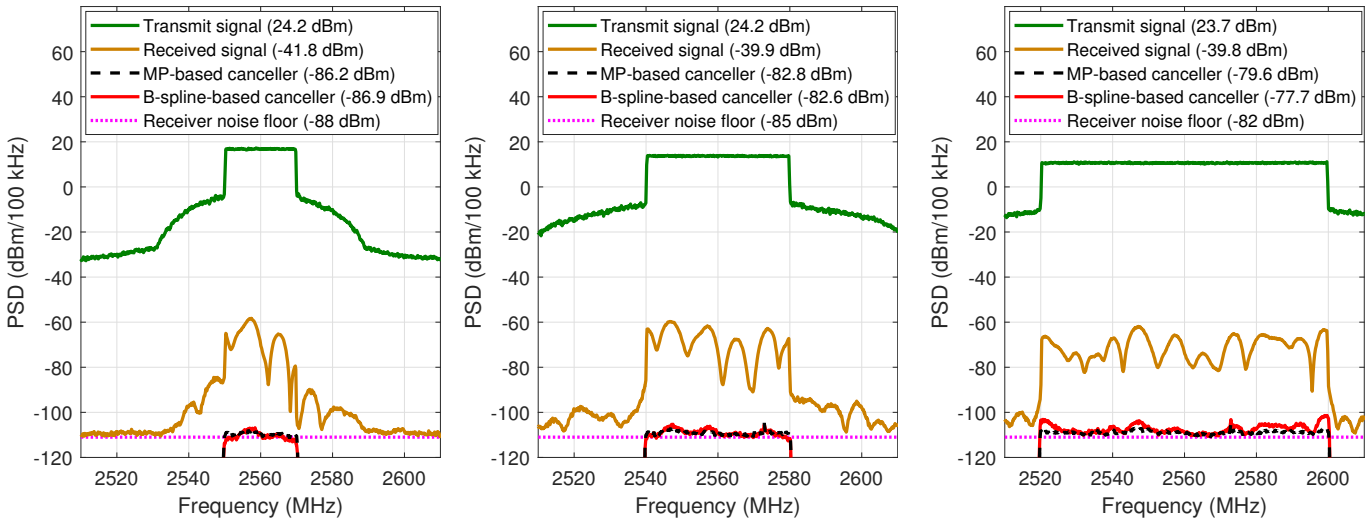

(a) (b) (c)

Fig. 4: PSDs of the overall signal after the different digital cancellers for (a) 20 MHz, (b) 40 MHz, and (c) 80 MHz instantaneous bandwidths.

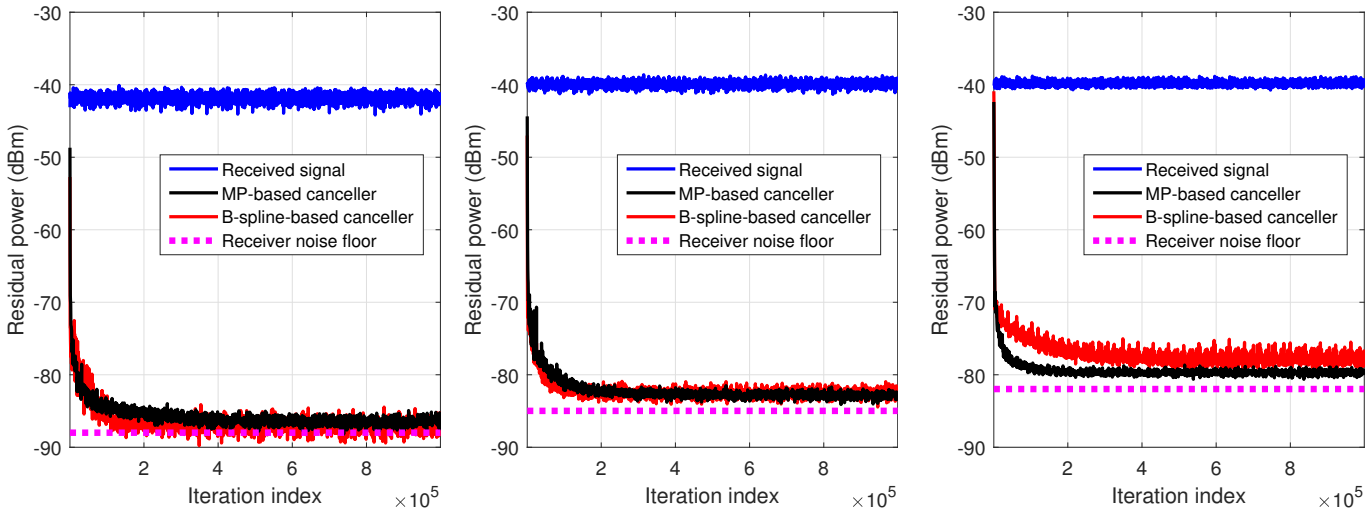

(a) (b) (c)

Fig. 5: Residual powers with respect to the iteration index after the different digital cancellers for (a) 20 MHz, (b) 40 MHz, and (c) 80 MHz instantaneous bandwidths.

is, the RF canceller is omitted altogether, as opposed to the more generic full-duplex transceiver architecture depicted in Fig. 1. Since this results in less SI suppression before the analog-to-digital conversion, a significant amount of digital cancellation is required, making this data ideal for evaluating the performance of the proposed digital canceller. The more detailed measurement parameters are listed in Table II.

First, the power spectral densities (PSDs) of the SI signal after the different stages of the full-duplex device are shown in Fig. 4. With instantaneous bandwidths of 20 MHz and 40 MHz, the spline-based canceller obtains essentially the same amount of cancellation as the MP-based canceller, despite the substantial complexity reduction. In these two cases, the amount of digital cancellation with the proposed canceller is 45 dB and 43 dB, respectively, which indicates very high modeling accuracy. Keeping in mind that it uses 77% fewer multiplications than the MP model, the complexity-accuracy trade-off of spline-based modeling is very intriguing. With the widest considered bandwidth of 80 MHz, the MP-based canceller outperforms the proposed digital canceller by some 2 dB. Therefore, further work is still needed to ensure sufficient modeling accuracy of splines under very wideband operation. It should be noted, however, that the proposed canceller can suppress the SI by 38 dB even over 80 MHz, which is in most cases sufficient cancellation performance.

To evaluate the convergence behavior of the proposed digital canceller, Fig. 5 shows the residual power after the two digital cancellers, using the same data as in Fig. 4. For the

TABLE II: The essential RF measurement parameters.

Parameter		Value
Center frequency		2.56 GHz
Bandwidth		20–80 MHz
Transmit waveform		OFDM
Transmit power		24 dBm
RX losses		4 dB
Parameter estimation sample size		1 000 000
MP-based canceller	M_{pre}	25
	M_{post}	50
	P_{MP}	11
Spline-based canceller	M_{pre}	25
	M_{post}	50
	P_{SP}	2
	Q	11

20-MHz and 40-MHz SI signals, it can be observed that the proposed spline-based digital canceller converges faster than the MP-based canceller, thereby reaching the steady-state sooner. However, in accordance with the observations made in Fig. 4, the 80-MHz case seems to be somewhat more challenging for the spline-based digital canceller also in terms of convergence behaviour. Figure 5c shows that the spline-based canceller converges somewhat slower than the MP-based canceller, while also suffering from slightly higher steady-state error. Nevertheless, these results prove that with bandwidths of 40 MHz or less, the proposed canceller can retain the highest possible cancellation performance while using significantly less computational resources.

V. Conclusion

In this paper we proposed a novel digital self-interference canceller for inband full-duplex devices that relies on splines and decoupled modeling when reconstructing nonlinearly distorted self-interference signals at digital baseband. To the best of our knowledge, this is the first time splines have been applied to self-interference cancellation. The benefit of the proposed approach is a significant reduction in the number of computations required within the digital canceller while still retaining high cancellation performance. In particular, it was shown that the proposed solution can obtain cancellation performance comparable to the existing state-of-the-art digital canceller while using 77% fewer multiplications per iteration. The measured digital self-interference cancellation numbers, obtained in a complete inband full-duplex radio prototype system operating at 2.4 GHz ISM band, are 45 dB, 43 dB and 38 dB with 20 MHz, 40 MHz and 80 MHz channel bandwidths, respectively. Therefore, the spline-based digital canceller is an important step towards commercially feasible inband full-duplex devices, where processing complexity and energy consumption are of fundamental importance.

Acknowledgment

This work was supported by the Academy of Finland (under the projects #304147 "In-Band Full-Duplex Radio Technology: Realizing Next Generation Wireless Transmission", and #301820 Competitive Funding to Strengthen University Research Profiles), the Finnish Funding Agency for Innovation (Tekes, under the projects "5G Transceivers for Base Stations and Mobile Devices (5G TRx)" and "TAKE-5"), Nokia Networks, RF360 Europe, Pulse, Sasken, and Huawei Technologies, Finland.

References

[1] M. Duarte, C. Dick, and A. Sabharwal, "Experiment-driven characterization of full-duplex wireless systems," *IEEE Transactions on Wireless Communications*, vol. 11, no. 12, pp. 4296–4307, Dec. 2012.

[2] D. Bharadia, E. McMilin, and S. Katti, "Full duplex radios," in *Proc. SIGCOMM'13*, Aug. 2013, pp. 375–386.

[3] D. Korpi, J. Tamminen, M. Turunen, T. Huusari, Y.-S. Choi, L. Anttila, S. Talwar, and M. Valkama, "Full-duplex mobile device: Pushing the limits," *IEEE Communications Magazine*, vol. 54, no. 9, pp. 80–87, Sep. 2016.

[4] D. Korpi, M. Heino, C. Icheln, K. Haneda, and M. Valkama, "Compact inband full-duplex relays with beyond 100 dB self-interference suppression: Enabling techniques and field measurements," *IEEE Transactions on Antennas and Propagation*, vol. 65, pp. 960–965, Feb. 2017.

[5] M. Chung, M. S. Sim, J. Kim, D. K. Kim, and C. b. Chae, "Prototyping real-time full duplex radios," *IEEE Communications Magazine*, vol. 53, no. 9, pp. 56–63, Sep. 2015.

[6] A. Sabharwal, P. Schniter, D. Guo, D. W. Bliss, S. Rangarajan, and R. Wichman, "In-band full-duplex wireless: Challenges and opportunities," *IEEE Journal on Selected Areas in Communications*, vol. 32, no. 9, pp. 1637–1652, Sep. 2014.

[7] D. Korpi, "Full-duplex wireless: Self-interference modeling, digital cancellation, and system studies," Ph.D. dissertation, Tampere University of Technology, Dec. 2017.

[8] M. Scarpiniti, D. Comminiello, R. Parisi, and A. Uncini, "Hammerstein uniform cubic spline adaptive filters: Learning and convergence properties," *Signal Processing*, vol. 100, pp. 112–123, 2014.

[9] C. De Boor, *A practical guide to splines*. Springer-Verlag New York, 1978.

[10] M. Scarpiniti, D. Comminiello, R. Parisi, and A. Uncini, "Nonlinear spline adaptive filtering," *Signal Processing*, vol. 93, no. 4, pp. 772–783, 2013.

[11] D. Korpi, Y.-S. Choi, T. Huusari, S. Anttila, L. Talwar, and M. Valkama, "Adaptive nonlinear digital self-interference cancellation for mobile inband full-duplex radio: algorithms and RF measurements," in *Proc. IEEE Global Communications Conference (GLOBECOM)*, Dec. 2015.

[12] D. P. Mandic and V. Su Lee Goh, *Complex Valued Nonlinear Adaptive Filters: Noncircularity, Widely Linear and Neural Models*. Wiley, 2009.

[13] A. S. Tehrani, H. Cao, S. Afsardoost, T. Eriksson, M. Isaksson, and C. Fager, "A comparative analysis of the complexity/accuracy tradeoff in power amplifier behavioral models," *IEEE Transactions on Microwave Theory and Techniques*, vol. 58, no. 6, pp. 1510–1520, 2010.

[14] M. Frerking, *Digital Signal Processing in Communications Systems*. Springer, 1994.